

# Predictions of Values in a Causticizing Process

R. Andreola, O. A. A. Santos, L. M. M. Jorge

**Abstract**—An industrial system for the production of white liquor of a paper industry, Klabin Paraná Papéis, formed by ten reactors was modeled, simulated, and analyzed. The developed model considered possible water losses by evaporation and reaction, in addition to variations in volumetric flow of lime mud across the reactors due to composition variations. The model predictions agreed well with the process measurements at the plant and the results showed that the slaking reaction is nearly complete at the third causticizing reactor, while causticizing ends by the seventh reactor. Water loss due to slaking reaction and evaporation occurs more pronouncedly in the slaking reaction than in the final causticizing reactors; nevertheless, the lime mud flow remains nearly constant across the reactors.

**Keywords**—Causticizing, lime, prediction, process.

## I. INTRODUCTION

ACCORDING to the Brazilian Association of Cellulose and Paper, BRACELPA [1] Brazil is one of the largest world producers of cellulose (4th) and paper (11th). In 2008, the cellulose and paper industry produced 114,000 direct jobs and 500,000 indirect jobs. In the last ten years (1999-2008), the production of cellulose paste rose from 7,209,132 tons to 12,696,546 tons, while the paper production rose from 6,953,246 tons to 9,409,450 tons, with increases of 76.1 and 35.3%, respectively [2].

This fast growth must continue in the future, mainly due to the high productivity of Brazilian planted forests and the low cost production in relation to other countries [3]. In addition to this characteristic of the sector in Brazil, the incorporation of new technologies and the application of computational tools tend to consolidate the growth and increase the economic advantages. Among the new technologies, the use of enzymes in pulp bleaching [4], [5] and the substitution of the conventional causticizing process by the selfcausticizing process are important [6], [7] which do not require the use of preset slaker reactors as in the conventional process. The use of computational tools to simulate, analyze, optimize, and control processes also already is a reality in the paper sector [8]-[14]. However, the development of these tools frequently faces the inexistence of appropriate and validated mathematical models.

In Brazil, the company Klabin S.A. produces most of the paper, and the state of Paraná is the second paper and cellulose producer [2]. In the kraft pulping process, the chemical

recovery step of causticizing which is utilized to regenerate the hydroxide, the main component of white liquor, has an impact on the operating cost of the kraft mill. A typical causticizing system consists of a slaker and a series or causticizers. The reactor system of Klabin Paraná Papéis that produces white liquor for the cellulose digesters consists of ten stirred tank reactors: a slaker reactor (SR) that is followed by a series arrangement of nine causticizing reactors, C1 to C9, as shown in Fig. 1. In this system, all the reactors are open at the top, operate at atmospheric pressure, and the last five reactors (C5-C9) are thermally isolated. Green liquor and lime are continually fed into the slaker reactor under stirring. Green liquor from the recovery boiler is basically a diluted  $\text{Na}_2\text{CO}_3$  aqueous solution, while the lime from the calcination kiln is predominantly calcium oxide and inert solids, around 11.5%. Lime immediately reacts with water when it is mixed with the green liquor in the slaker reactor, forming calcium hydroxide through the highly exothermal slaking reaction:  $\text{CaO}_{(s)} + \text{H}_2\text{O}_{(l)} \rightarrow \text{Ca}(\text{OH})_{2(s)}$ . In turn, calcium hydroxide simultaneously reacts with sodium carbonate in the green liquor to form sodium hydroxide and calcium carbonate through the slightly exothermal reaction:  $\text{Na}_2\text{CO}_{3(aq)} + \text{Ca}(\text{OH})_{2(s)} \rightarrow 2 \text{NaOH}_{(aq)} + \text{CaCO}_{3(s)}$ . Two distinct streams leave the reactor outlet: grits and lime mud. The grit stream is constituted of inert solids in lime sedimented at the bottom of the reactor and driven out through the reactor outlet by an inclined endless screw for disposal. The lime mud stream is mostly constituted of unreacted suspended solids and  $\text{NaOH}$  and  $\text{Na}_2\text{CO}_3$ , in aqueous solution.

The suspended solids are formed by the inert substances, such as  $\text{CaCO}_3$ , residual reagents, such as  $\text{Ca}(\text{OH})_2$ ,  $\text{CaO}$ , and a percent of grits dragged by the lime mud stream. After leaving the slaker reactor, the lime mud stream sequentially runs through the series of nine causticizing reactors (C1-C9) to provide the necessary residence time for the causticizing reaction to complete. The usual residence times ( $\tau_i = V_i/q_i$ ) are shown in Table I. Klabin Paraná Papéis is located in the city of Telêmaco Borba, in Paraná State, south Brazil. It produces paper and cellulose from pine and eucalyptus wood from its own reforestation cultures. The overall performance of a causticizing system is affected by various factors, such as the quality and quantity of lime, the concentration of the green liquor components, temperature, and mixing intensity [15]. In this sense, the determination of the optimal operating conditions and the possibility of using suitable control systems will contribute to improve the system performance and economy. Both the control and the analysis of the process and the optimization of the operating conditions can be carried out through the development and validation of appropriate mathematical modeling. Reference [16] developed static and

R. Andreola is with the Centro Universitário de Maringá, UniCesumar, Bloco 07, Avenida Guedner, 1610, Jardim Aclimação, 87050-900, Maringá, Paraná, Brazil (corresponding author; ricardo.andreola@unicesumar.edu.br).

L. M. M. Jorge and O. A. A. Santos are with the Universidade Estadual de Maringá - UEM, Departamento de Engenharia Química, Campus Universitário, Av. Colombo, 5790, Bloco D90, 87020-900, Maringá, Paraná, Brazil.

dynamic models for a causticizing plant and lime kiln; however, the level of details given is insufficient. Apparently, it is a black box-type empirical model. It is not possible to prove the use of industrial data in the validation of the models or their applicability. According to the authors, the dynamic models were used with success in a novel control system of both the causticizing plant and the lime kiln.

TABLE I  
USUAL RESIDENCE TIMES

Reactor	SR	C1	C2	C3, C4	C5,C6	C7 to C9
$\tau$ (s)	1051	1387	1386	1385	1437	1493

Reference [17] successfully automated an industrial causticizing process by applying an adaptive control system. They overcame the inexistence of a duly identified phenomenological model by using a black box-type transfer function based on a series of Laguerre's orthogonal functions, while [18] presented one of the few studies in the literature involving the dynamic phenomenological modeling and the validation with industrial data for a conventional causticizing process. The authors developed a phenomenological model based on unsteady-state material and energy balances in the slaker and causticizing reactors and by admitting constant volume, perfect mixture, and apparent concentrations. In this model, the causticizing reaction speed was obtained by adding a  $\text{Ca}(\text{OH})_2$  concentration term to the empirical kinetics equation to account for the influence of the added amount of lime [19], while the slaking reaction rate was approximated by a first order reaction rate expression.

Other study [20] analyzed the effect of water loss by evaporation and chemical reaction in an industrial slaker reactor operating in steady state. They developed a dynamic model using an approach similar to that used by [18]. Among the main differences are the uses of actual concentrations instead of apparent concentrations by subtracting the volume of solids in suspension in the calculation of the concentrations and the estimate of the global coefficient value from a U phenomenological model based on the association of thermal resistances. The predictions of this model in steady state satisfactorily represented the experimental temperature measures, active alkali (AA) and total titrable alkali (TTA), without parameter fitting. In this context, this work sought to model, simulate, and analyze the whole liquor reactor system of Klabin Paraná Papéis (Fig. 1). Mathematical models were developed for nine causticizing reactors using the same approach adopted by [20]. The models were numerically resolved with the concepts of apparent and actual concentrations, and the simulation results were compared to each other and with the plant measurements of temperature, AA and TTA.

## II. MATHEMATICAL MODELING

The causticizing reactor system shown in Fig. 1 is divided in two distinct parts: a slaker reactor and nine causticizing reactors. The causticizing reactors C1 to C9 are analyzed in

this work in the same process operating conditions that the slaker reactor was previously modeled and simulated by [20].

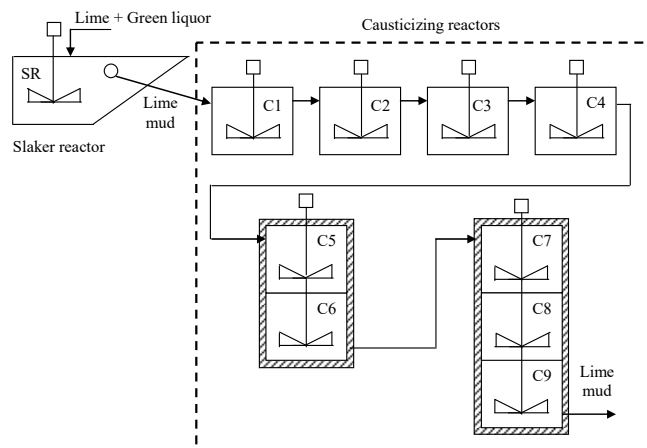


Fig. 1 Klabin Paraná Papéis reactor system

The causticizing reactor mathematical model was obtained by mass balancing each component for a generic reactor  $i$ , according to (1) to (7), and energy balancing (9), based on causticizing reactor  $i$ . It was considered a perfect mixture and constant volume, water loss by evaporation, and variations in the volumetric flow of lime mud at the reactor outlet due to the production of carbonate and calcium hydroxide and the consumption of water and calcium oxide by the slaking and causticizing reactions.

$$\frac{dC_{a,i}^*}{dt} = \frac{1}{V_i} (q_{i-1} C_{a,i-1}^* - q_i C_{a,i}^*) - r_1 \left( \frac{PM_a}{PM_{Na_2O}} \right) \quad (1)$$

$$\frac{dC_{b,i}^*}{dt} = \frac{1}{V_i} (q_{i-1} C_{b,i-1}^* - q_i C_{b,i}^*) + 2r_1 \left( \frac{PM_b}{PM_{Na_2O}} \right) \quad (2)$$

$$\frac{dC_{c,i}^*}{dt} = \frac{1}{V_i} (q_{i-1} C_{c,i-1}^* - q_i C_{c,i}^*) \quad (3)$$

$$\frac{dm_{d,i}}{dt} = \frac{m_{d,i-1}}{V_{i-1}} q_{i-1} - \frac{m_{d,i}}{V_i} q_i - V_i r_2 \quad (4)$$

$$\frac{dm_{e,i}}{dt} = \frac{m_{e,i-1}}{V_{i-1}} q_{i-1} - \frac{m_{e,i}}{V_i} q_i - V_i \left( \frac{PM_e}{PM_{Na_2O}} \right) r_1 + V_i \left( \frac{PM_e}{PM_d} \right) r_2 \quad (5)$$

$$\frac{dm_{f,i}}{dt} = \frac{m_{f,i-1}}{V_{i-1}} q_{i-1} - \frac{m_{f,i}}{V_i} q_i + V_i \left( \frac{PM_f}{PM_{Na_2O}} \right) r_1 \quad (6)$$

$$\frac{dm_{g,i}}{dt} = \frac{m_{g,i-1}}{V_{i-1}} q_{i-1} - \frac{m_{g,i}}{V_i} q_i \quad (7)$$

where: a –  $\text{Na}_2\text{CO}_3$ ; b –  $\text{NaOH}$ , c –  $\text{Na}_2\text{S}$ ; d –  $\text{CaO}$  and –  $\text{Ca}(\text{OH})_2$ ; f –  $\text{CaCO}_3$ ; g – inert solids.

The supposition of a perfect mixture is grounded on [25], which demonstrated that the distribution of the residence time of solids is equal to that of the liquid in a causticizing reactor system. The balance of components a, b, and c was deduced in terms of apparent concentrations ( $C_a^*$ ,  $C_b^*$ ,  $C_c^*$ ). These concentrations represent the mass of a given dissolved component per reactor volume unit (RVU). However, in strict sense, these concentrations do not represent their actual concentrations in the liquid phase of the reaction mixture, as part of the reactor volume is filled with solids.  $\text{CaCO}_3$ ,  $\text{CaO}$ ,  $\text{Ca(OH)}_2$  and inert solids from the lime added to the slaker reactor must have their volumes subtracted for evaluating the actual concentration of the component in the solution. In this way, the actual concentration of a generic component i ( $C_i$ ) was determined from its apparent concentration ( $C_i^*$ ) using (8).

$$C_i = C_i^* \left( \frac{V_i}{V_r} \right) \quad (8)$$

where:

$$V_r = V_i - \left( \frac{m_{f,i}}{\rho_f} + \frac{m_{e,i}}{\rho_e} + \frac{m_{d,i}}{\rho_d} + \frac{m_{g,i}}{\rho_g} \right)$$

The operating temperatures of the first causticizing reactors are very close to the boiling point of the reaction mixture. Additionally, the reactions involved in the process are exothermal, which favors the increase of the medium temperature. In this way, it was computed the energy loss by evaporation ( $q_{\text{evap}}$ ) in the energy balance in (9). For further details, see [21].

$$\frac{dT_i}{dt} = C_1 - q_{\text{evap}} C_2 \quad (9)$$

where:

$$C_1 = \frac{1}{V_i \rho_{\text{mud}} C_{p_{\text{mud}}}} [\Delta H_{\text{mud}} + \Delta H_{\text{solid}} + (-\Delta H_1) V_i r_1 + (-\Delta H_2) V_i r_2 - UA_i (T_i - T_{\text{amb}})];$$

$$C_2 = \frac{\rho_{\text{H}_2\text{O}} \Delta H_{\text{evap}}}{V_i \rho_{\text{mud}} C_{p_{\text{mud}}}}$$

As the reactor temperature (T) was lower than the boiling temperature of the reaction mixture ( $T_{\text{eb}}$ ), evaporation was dismissed, therefore,  $q_{\text{evap}} = 0$ . However, as soon as the reactor temperature reaches  $T_{\text{eb}}$ , water will evaporate at constant temperature. The evaporation rate ( $q_{\text{evap}}$ ) was evaluated instantaneously with the following expression:  $C_1 - q_{\text{evap}} C_2 = 0$ . As previously mentioned, the lime mud stream is basically formed by an aqueous solution of sodium hydroxide with carbonate and calcium hydroxide, inert solids, and occasionally unreacted calcium oxide in suspension. Consequently, the lime mud volumetric flow inside reactor i ( $q_i$ ) is constituted by the sum of five distinct components: water ( $q_{\text{H}_2\text{O}}$ ), calcium carbonate ( $q_{\text{CaCO}_3}$ ), calcium hydroxide

( $q_{\text{Ca(OH)}_2}$ ), calcium oxide ( $q_{\text{CaO}}$ ), and inert solids ( $q_{\text{inert}}$ ), as shown in (10):

$$q_i = q_{\text{H}_2\text{O},i} + q_{\text{CaCO}_3} + q_{\text{Ca(OH)}_2} + q_{\text{CaO}} + q_{\text{inert}} \quad (10)$$

where:

$$q_{\text{CaCO}_3} = q_i \left( \frac{m_{f,i}}{V_i \rho_f} \right); \quad q_{\text{Ca(OH)}_2} = q_i \left( \frac{m_{e,i}}{V_i \rho_e} \right); \quad q_{\text{CaO}} = q_i \left( \frac{m_{d,i}}{V_i \rho_d} \right);$$

$$q_{\text{inert}} = q_i \left( \frac{m_{g,i}}{V_i \rho_g} \right)$$

In turn, the volumetric flow of water ( $q_{\text{H}_2\text{O}}$ ) can be calculated from its mass balance considering a pseudo stationary behavior, evidencing the water consumption in the slaking reaction ( $q_{\text{reaction}}$ ) and loss by evaporation ( $q_{\text{evap}}$ ), such as given in (11):

$$q_{\text{H}_2\text{O},i} = q_{\text{H}_2\text{O},i-1} - q_{\text{reaction}} - q_{\text{evap}} \quad (11)$$

where:

$$q_{\text{reaction}} = \frac{r_1 V_i}{\rho_{\text{H}_2\text{O}}} \left( \frac{PM_{\text{H}_2\text{O}}}{PM_{\text{Na}_2\text{O}}} \right)$$

Combining (10) and (11) gives the volumetric flow of lime mud at the outlet of causticizing reactor i,  $q_i$ , (12):

$$q_i = \left( \frac{V_i}{V_r} \right) (q_{i-1} - q_{\text{reaction}} - q_{\text{evap}}) \quad (12)$$

The reaction speed equations for slaking ( $r_2$ ),  $\text{CaO}_{(s)} + \text{H}_2\text{O}_{(l)} \rightarrow \text{Ca(OH)}_{2(s)}$ , and causticizing ( $r_1$ ),  $\text{Na}_2\text{CO}_{3(aq)} + \text{Ca(OH)}_{2(s)} \rightarrow 2\text{NaOH}_{(aq)} + \text{CaCO}_{3(s)}$ , employed in this work are those used by [22], showed in (13) and (14), respectively:

$$r_2 = k_2 \left( \frac{m_{d,i}}{V_i} \right) \quad (13)$$

$$r_1 = \left( \frac{PM_{\text{Na}_2\text{O}}}{PM_a} \right) C_{a,i-1}^* \left( \frac{m_{e,i}}{V_i} \right) A \quad (14)$$

where:

$$A = \left\{ k_1 C_{a,i}^* \left( \frac{PM_{\text{Na}_2\text{O}}}{PM_a} \right) - k_1 [EA]^2 \right\}$$

$$EA = C_b^* \frac{PM_{\text{Na}_2\text{O}}}{PM_b} + 0,5 C_c^* \frac{PM_{\text{Na}_2\text{O}}}{PM_c}$$

### III. NUMERICAL SOLUTION

The mathematical model described above was numerically solved by integrating the model differential equation system sequentially with subroutine SDRIV2, which is available at [23], that is: causticizing reactor 1 (C1) was simulated by admitting that initially it is in the same conditions as the slaker

reactor is in steady state conditions. Next C2 was simulated by admitting that it was initially in the same conditions as those of C1 at steady state, and so forth until the last reactor (C9). It is worth pointing out that the initial conditions of simulation of C1 were obtained from steady state values reported by [20] for the operation of the slaker reactor of the system depicted in Fig. 1 operating in steady state.

#### IV. EVALUATION OF THE MODEL PARAMETERS

The mathematical model has a thermal parameter, U, and three apparent kinetic parameters:  $k_2$ ,  $k_{1,0}$ , and  $k_{2,0}$ . The kinetic parameters used are those employed by [22], while the global parameters of causticizing reactors C1 to C4 were estimated with (15) in [24], as described by [20]. These values were considered null for causticizing reactors C5-C9, as they are thermally isolated, as shown in Fig. 1. All the parameter values used in the simulations are presented in Table II.

$$\frac{1}{UA} = \frac{1}{h_{ext}A} + \frac{e}{A_m k_w} + \frac{1}{h_{int}A} \quad (15)$$

TABLE II  
THERMAL AND KINETIC PARAMETERS

Reactor	U (J/K.m.s)	$k_2$ (s <sup>-1</sup> )	$k_{1,0}$ (-)	$k_{2,0}$ (-)
C1 - C4	6.2790	$5.55 \cdot 10^{-3}$	950.0	5.95
C5 - C6	0.0	$5.55 \cdot 10^{-3}$	950.0	5.95
C7 - C9	0.0	$5.55 \cdot 10^{-3}$	950.0	5.95

$$* k_1 = k_{1,0} \exp[-9.5 \cdot 10^{-2} (TTA - 112.33) - 27190 / RT]$$

$$** k_1 = k_{2,0} \exp[-6.04 \cdot 10^{-2} (TTA - 112.33) - 23004.14 / RT]$$

#### V. RESULTS AND DISCUSSION

Figs. 2-10 give the results of the simulations for SR and C1 to C9 in steady state. The analysis of Figs. 2-4 reveals that the simulations made based on the apparent concentration concept resulted in values lower than those obtained using the actual concentration concept, which is due to the use of only the actual liquid volumes in the reactors in the calculations of the actual concentrations, while in the case of the apparent concentrations, the solid and liquid volumes were considered together, thus giving a lower value for the apparent concentration of the component.

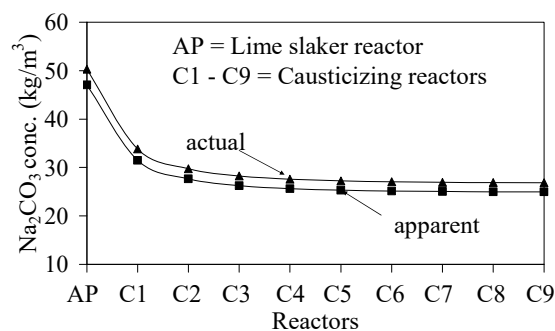


Fig. 2 Na<sub>2</sub>CO<sub>3</sub> concentration

In a similar way, both the active alkali (AA) values and the total titrable alkali (TTA) obtained from the apparent concentrations were also lower than the values obtained from the actual steady state conditions, as can be seen in Figs. 5 and 6.

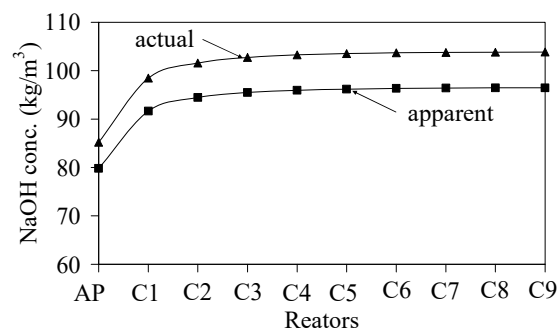


Fig. 3 NaOH concentration

The comparison of the AA and TTA experimental measures, free of solids in suspension and in steady state, leads to the conclusion that the actual concentration concept results are closer to the experimental values, indicating its preferential use.

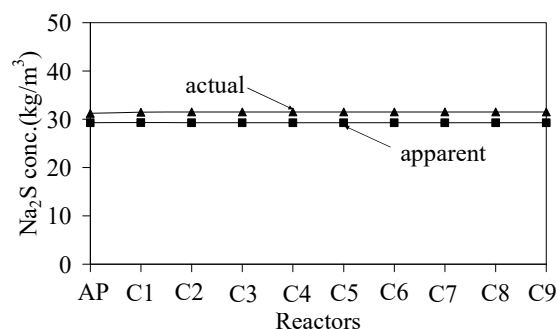


Fig. 4 Na<sub>2</sub>S concentration

The fact that the active alkali increased up to C2, Fig. 5, and it is stabilized from C3 on indicates that the causticizing reaction occurs more pronouncedly up to C3 without further significant effect in the subsequent reactors.

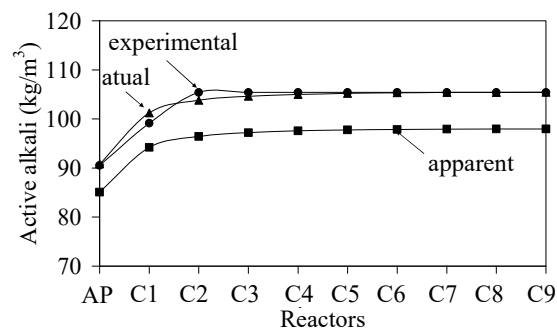


Fig. 5 Active alkali (AA)

A possible explanation for the nearly invariable TTA values in the causticizing reactors, Fig. 6, is that TTA consists of the

concentrations of components  $\text{Na}_2\text{CO}_3$ ,  $\text{NaOH}$ , and  $\text{Na}_2\text{S}$ , relative to the same base ( $\text{Na}_2\text{O}$ ).

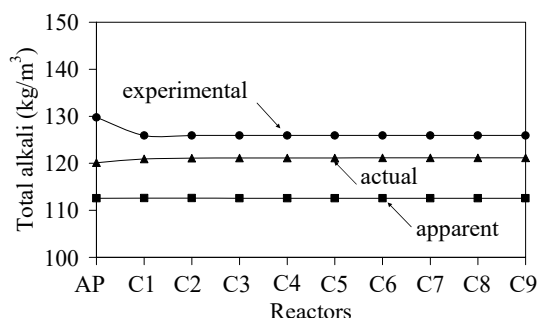


Fig. 6 Total alkali (TTA)

Thus, the TTA value remains constant because an increase in the  $\text{NaOH}$  concentration results in a decrease in the  $\text{Na}_2\text{CO}_3$  concentration because of the causticizing reaction, compensating each other, while the concentration of  $\text{Na}_2\text{S}$  remains constant, Fig. 4, as it does not participate in the slaking and causticizing reactions.

The analysis of the mass simulations of  $\text{Ca}(\text{OH})_2$  per RVU in steady state conditions given in Fig. 7 shows a high consumption of  $\text{CaO}$  in the slaking reactions in C1 and that it tended to zero in C3.

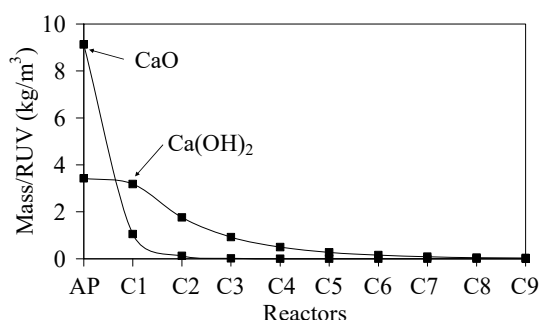


Fig. 7  $\text{CaO}$  and  $\text{Ca}(\text{OH})_2$  masses

In turn, the mass of  $\text{Ca}(\text{OH})_2$  per RVU also decreased across the causticizing reactors due to its increased consumption, in contrast to the total  $\text{CaO}$  mass, which slowly decreased in the first reactors and tended to a negligible value only after C7, showing that the causticizing reaction speed was much smaller than the slaking reaction speed.

Calcium hydroxide is produced in the slaking reaction from calcium oxide and consumed in the causticizing reaction, producing calcium carbonate, so that the  $\text{Ca}(\text{OH})_2$  mass in the reactors at any instant results from the competition between these two reactions. Fig. 7 shows that the  $\text{CaO}$  mass quickly decreased after the slaking reactor, tending to null close to C3, which indicated the end of the slaking reaction. In contrast, the  $\text{Ca}(\text{OH})_2$  mass became null only around C7, characterizing a smaller reaction speed and the end of the causticizing reaction. Therefore, it was observed that the reactor system analyzed is overdimensioned and that the last two reactors, C8 and C9, are redundant. This allows for an increase in the white liquor production without an expansion of the current reactor system.

The calcium carbonate mass increased significantly in the first three causticizing reactors and to a lesser extent in the subsequent reactors, as shown in Fig. 8.

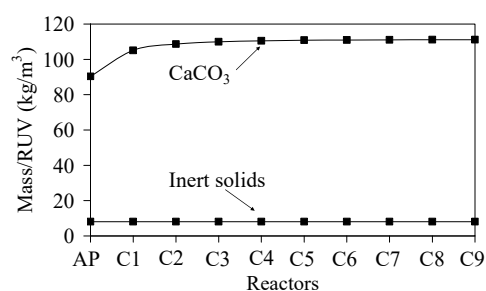


Fig. 8  $\text{CaCO}_3$  and inert solid masses

In contrast, the inert solid mass remained constant across all reactors, as it resulted from the inert solids in the lime added to the slaking reactor. Similarly for AA and TTA, the mathematical model explained the thermal behavior of the system satisfactorily in steady state conditions. As can be observed in Fig. 9, the largest difference between the simulation and the experimental values was in the order of  $2^\circ\text{C}$  in C9. It can also be noted that the simulation temperature remained at  $100^\circ\text{C}$  from C1 to C3, decreasing to  $99.6^\circ\text{C}$  in C4 and remaining nearly stable throughout to C9.

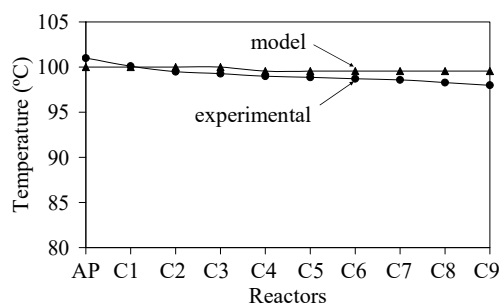


Fig. 9 Temperature in steady state

The lime mud volumetric flow across the causticizing reactors ( $q_i$ ) was influenced mainly by the water ( $q_{\text{H}_2\text{O}}$ ) and secondarily by the calcium carbonate ( $q_{\text{CaCO}_3}$ ), and in negligible form by the calcium oxide and hydroxide ( $q_{\text{CaO}}$ ,  $q_{\text{Ca}(\text{OH})_2}$ ) and inert solid ( $q_{\text{Inert}}$ ), as shown in Fig. 10.

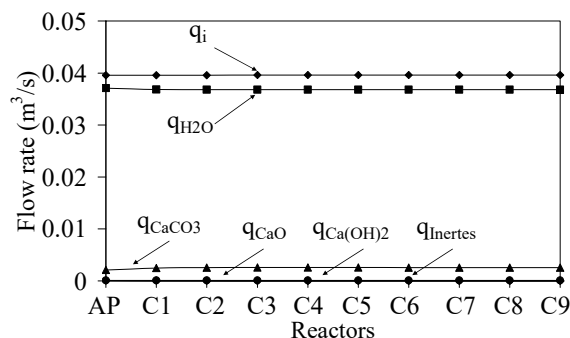


Fig. 10 Total lime mud flow,  $q_i$

The difference between the total  $q_i$  and  $q_{H_2O}$  flows at the outlet of C9 is in the order of 7.10%, almost entirely due to the production of calcium carbonate in the causticizing reaction.

Water is the main constituent of lime mud. However, the water content of this stream ( $q_{H_2O}$ ) can be affected by both the water consumption in the slaking reaction ( $q_{r1}$ ) and by water loss by evaporation ( $q_{evap}$ ), in agreement with (11). The analysis of Fig. 11 shows that water loss by both evaporation and in the slaking reaction was significant only in the slaking reactor, being negligible in the other reactors (C1 to C9), which makes the difference between the water flow input ( $q_{H_2O,i}$ ) and output ( $q_{H_2O,o}$ ) of the causticizing reactors null.

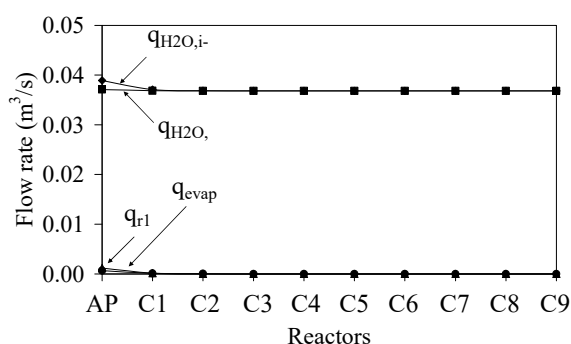


Fig. 11 Water flow rate,  $q_{H_2O}$

## VI. CONCLUSIONS

- The developed model simulated the behavior of the industrial causticizing reactors in steady state satisfactorily, not requiring any parameter fitting.
- The use of the actual concentration concept is indicated for modeling the white liquor reactor system.
- The difference between the actual and apparent concentrations of  $Na_2CO_3$ ,  $NaOH$ , and  $Na_2S$  is significant, with a mean value of 7.0%.
- The causticizing reaction is much slower than the slaker reaction.
- The difference between the lime mud and water flow at the causticizing reactor system outlet is about 7.1% and it results mainly from the calcium carbonate present in the lime mud suspension.
- In steady state conditions, the slaking reaction is nearly completed in C3, the fourth system reactor, while the causticizing reaction is completed in about the eighth reactor, C7.
- In the operating conditions investigated, the reactor system analyzed is overdimensioned, making the last two reactors, C8 and C9 redundant, which allows for an increase in the white liquor production without an expansion of the current reactor system.

## NOMENCLATURE

A	area, m <sup>2</sup>
AA	active alkali, such as Na <sub>2</sub> O, kg/m <sup>3</sup>
C	concentration, kg/m <sup>3</sup>
C <sub>p</sub>	heat capacity, J/(kg.K)
E	activation energy, J/gmol

e	reactor wall thickness, m
EA	effective alkali, such as Na <sub>2</sub> O, kg/m <sup>3</sup>
H	heat transfer coefficient, J/(K.s.m <sup>2</sup> )
H	causticizing reaction enthalpy, J/kgNa <sub>2</sub> O; slaking reaction enthalpy, J/kgCaO
k	thermal conductivity, J/(s.m.K), or relative to kinetic parameters
m	mass, lb
PM	molecular weight
q	volumetric flow, m <sup>3</sup> /s
R	ideal gas constant, J/(gmol.K)
r	reaction speed, kgNa <sub>2</sub> O/(m <sup>3</sup> .s) for the causticizing reaction, and kgCaO/(m <sup>3</sup> .s) for the slaking reaction
T	temperature, °C
TTA	total titrable alkali, such as Na <sub>2</sub> O, kg/m <sup>3</sup>
U	global heat transfer coefficient J/(K.m <sup>2</sup> .s)
V	operating volume, m <sup>3</sup>

## A. Greek Symbols

$\Delta$	variation
$\rho$	fluid density, lb/ft <sup>3</sup>
$\tau$	residence time, s

## B. Subscripts

eb	boiling
evap	evaporation
ext	external
in	reactor inlet
int	internal
mud	liquor and lime mud suspension
lm	logarithmic mean
w	wall
i	relative to the reactor number
1	relative to the causticizing reaction
2	relative to the slaking reaction

## ACKNOWLEDGMENTS

The authors thank the technical and financial support from Universidade Estadual de Maringá and Klabin Paraná Papéis.

## REFERENCES

- [1] BRACELPA - Associação Brasileira de Celulose e Papel (2009a). Desempenho do setor e projeções. <www.bracelpa.org.br/bra/estatisticas/pdf/booklet/booklet.pdf>, (accessed 10.02.10).
- [2] BRACELPA - Associação Brasileira de Celulose e Papel (2009b). Relatório Anual 2008/2009. <www.bracelpa.org.br/bra/estatisticas/pdf/rel2008.pdf>, (accessed 10.02.10).
- [3] Soares, N. S.; Silva, M. L.; Lima, J. E.. (2007), A função de produção da indústria brasileira de celulose, em 2004. *Rev. Árvore*, 31 (3), 495-502.
- [4] Medeiros, R. G.; Silva Jr., F. G.; Bão, S. N.; Hanada, R.; Ferreira Filho, E. X. (2007), Application of Xylanases from Amazon Forest Fungal Species in Bleaching of Eucalyptus Kraft Pulp. *Braz. Arch. Biol. Techn.*, 50 (2), 231-238.
- [5] Vilkari, L.; Kantelinen, A.; Linko, M. (1994), Xylanases in bleaching: from an idea to industry. *FEMS Microbiol. Rev.*, 13, 335-355.
- [6] Gonçalves, E. C.; Silva, C. M.; Alves, L. J. L.; Gomide, J. L.; Carneiro, C. J. G. (2008), Sodium metaborate auto-causticizing for eucalyptus kraft-antraquinone pulp production. *O Papel*, 4, 42-50.
- [7] Zeng, L., van Heiningen, A. R. P., A Mathematic Model for Direct Causticization of Na<sub>2</sub>CO<sub>3</sub> with TiO<sub>2</sub> in a Semi-batch Reactor. *Can. J. Chem. Eng.*, 80, 948-953, 2002.
- [8] Andrade, A. A.; Sartori, C. R. F.; Costa, V. L.; Freitas, M.; Rothen, T.; d'Angelo (2009), Implementation of advanced control and optimization in the causticizing process. *O Papel*, 70, 11, 66-77.
- [9] Lopes, R.; Fleet, V. R.; Figueiredo, D. (2008), Multivariable process control applications for the pulp industry. *O Papel*, 69 (11), 75-86.

- [10] Silva, F. A.; Restrepo, A.; Rodrigues, L. A.; Gedraite, R. (2008), Variability reduction and efficiency increase in lime kilns using advanced process control. *O Papel*, 69 (12), 75-85.
- [11] Malberg, B., Edwards, L. (2007), Dynamic modeling of pressurized peroxide stages with application to full bleach plant simulation. *Tappi J.*, 6 (2), 9-17.
- [12] Barber, V. A., Scott, G. M. (2007), Dynamic modeling of a paper machine, part I: programming and software development. *Tappi J.*, 6 (1), 11-17.
- [13] Aguiar, H. C.; Maciel Filho, R. (2001), Neuronal network and hybrid model: a discussion about different modeling techniques to predict pulping degree with industrial data. *Chem. Eng. Sci.*, 56, 565- 570.
- [14] Costa, A. O. S.; Biscaia Jr., E. C.; Lima, E. L. (2004), Mathematical description of the kraft recovery boiler furnace. *Comput. Chem. Eng.*, 28, 633-641.
- [15] Sethuraman, J.; Krishnagopalan, J.; Krishnagopalan, G. (1995), Kinetic model for the causticizing reaction. *Tappi J.*, 78 (1), 115-120.
- [16] Uronen, P.; Aurasmaa, H. (1979), Modelling and simulation of causticization plant and lime kiln. *Pulp Pap-Canada*, 80 (6), 162-165.
- [17] Andrade, A. A.; Sartori, C. R. F.; Costa, V. L.; Freitas, M.; Rothen, T.; d'Angelo (2009), Implementation of advanced control and optimization in the causticizing process. *O Papel*, 70, 11, 66-77.
- [18] Swanda, A. P.; Seborg, D. E.; Holman, K. L.; Sweerus, N. (1997), Dynamic models of the causticizing process. *Tappi J.*, 80 (12), 123-134.
- [19] Holman, K. L.; Warrick, R. P.; Carlson, K. R. (1991), Reausticizing kinetics with mill liquor and lime. *AIChE Forest Products Symposium Proceedings, AIChE*, NewYork, 23-31.
- [20] Andreola, R.; Vieira, O.; Santos, O. A. A.; Jorge, L. M. M. (2007), Effect of Water Losses by Evaporation and Chemical Reaction in an Industrial Slaker Reactor. *Braz. Arch. Biol. Techn.*, 50 (2), 339-347.
- [21] Andreola, R. (2001), Modeling, Simulation and Analysis of Klabin Paraná Papéis Causticizing Reactor System. M.S. Thesis (in Portuguese), State University of Maringá, Maringá, Brazil.
- [22] Swanda, A. P. (1994), Process modeling and control system evaluation for the pulp and paper reconstituting process. M.S. Thesis, University of California, USA.
- [23] Kahaner, D. Moler, C. Nash, S. (1989), *Numerical methods and software*. Prentice Hall Series in Computational Mathematics, New Jersey.
- [24] Lydersen, L. A. (1979), *Fluid flow and heat transfer*. John Wiley and Sons, New York.
- [25] Hypponen, O. and Luuko A. (1984), The residence time distributions of liquor and lime mud flows in the reconstituting process. *Tappi Journal*, 67:7, 46-48.